FROM PS TO FS: DEPENDENCE OF THE MATERIAL REMOVAL RATE AND THE SURFACE QUALITY ON THE PULSE DURATION FOR METALS, SEMICONDUCTORS AND OXIDES

Paper M1004

Beat Neuenschwander, Beat Jaeggi and Marc Schmid

[1] Bern University of Applied Science, Institute of Applied Laser, Photonics and Surface Technologies, Pestalozzistrasse 20, 3400 Burgdorf, Switzerland

Abstract

Ultra short laser pulses in the ps or fs regime are used, when high requirements concerning machining quality are demanded. However, beside the quality also the process efficiency denotes a key factor for the successful transfer of this technology into real industrial applications and the process efficiency is mainly influenced by the removal rate. In this work the results of a study about the influence of the pulse duration onto the removal rate for pulses from 10 *ps* down to 250 *fs* will be presented. The investigated materials were copper, stainless steel, silicon, germanium, zirconium oxide (ZrO_2), polycrystalline diamond (PCD) fused silica and soda lime glass. An increase of the removal rate with shorter pulse durations was observed for all materials except the two glasses. A very special behaviour with a sharp change between two regimes with different ablation processes was observed for soda lime glasses for both wavelengths.

Introduction

Ultra short pulsed systems show clear advantages concerning machining quality, heat affected zone, debris, etc [1-4]. But even if the excellent machining quality is one of the key advantages of ultra short pulsed systems, it may be more cost effective to use a Q-Switched system and to accept the reduced quality and additional costly post processing steps. One possibility to further increase the competitiveness of ultra short pulsed systems may be the change to fiber based amplifier technologies. Without CPA technology the pulse duration of these systems is expected to be in the range of several tens ps [5-7]. For metals the ablation efficiency significantly drops by about a factor of 5 when the pulse duration is raised from 10 *ps* up to 50 *ps* [8,9], for non metals this drop is less pronounced but still present [10]. The characteristics of the measured ablation efficiency as a function of the pulse duration implies, that the efficiency could increase when the pulse duration is reduced from 10 *ps* into the sub ps regime. Results corroborating this belief have been reported in [11-13]. For dielectrics in [14] an increase of the efficiency is reported when the pulse duration is reduced 300 *fs* – 7 *fs*. This all encourages the development of fiber based ultra short pulsed systems in the fs-regime which can be driven to high average powers by succeeding amplifier stages; recently more than 1 *kW* average power with fs – laser pulses were demonstrated [15,16]. From this point of view sub – ps systems could to be very attractive for laser micro processing.

Ablation Model

Theory

For ultra short pulses the heat-transfer process in metals is described with the two temperature model [1,17-21] where the temperatures of the electrons and the lattice are treated separately. The results of the model and the experiments show, that the ablation depth z_{abl} can be written as a function of the fluence ϕ (pulse energy per unit area):

$$z_{abl} = \delta \cdot \ln\left(\frac{\phi}{\phi_{th}}\right) \qquad (1)$$

with ϕ_{th} the threshold fluence and δ the energy penetration depth. Frequently two different ablation regimes are reported [19,22]: firstly the low fluence regime where the optical penetration depth dominates and secondly the high fluence regime where the energy transport is dominated by the heat diffusion of the hot electrons. In [23] it is shown, that for a top hat beam the efficiency of the ablation process depends on the ratio between the threshold fluence and the applied fluence ϕ_{th}/ϕ. The efficiency shows a maximum value of 1/e, i.e. about 37%. At this point of maximum efficiency the ablated volume per pulse reads:

$$\Delta V_{Pulse} = \pi \cdot w_0^2 \cdot \delta \qquad (2)$$

From this one can calculate the maximum removal rate per average power which reads for a top hat beam:

$$\frac{\dot{V}_{\max}}{P_{av}} = \eta_{\max} \cdot \frac{\delta}{\phi_{th}} = \frac{1}{e} \cdot \frac{\delta}{\phi_{th}} \tag{3}$$

The removal rate finally depends on the energy penetration depth δ and the threshold fluence ϕ_{th}.

Ablation for a Gaussian beam

Similar calculations have been done for a Gaussian shaped beam as emitted by most ultra short pulsed systems [24,25]. Again a maximum removal rate per average power (ablation efficiency) is observed:

$$\frac{\dot{V}_{\max}}{P_{av}} = \frac{2}{e^2} \cdot \frac{\delta}{\phi_{th}} \tag{4}$$

The ablated volume per pulse at this optimum points is again given by (2) i.e. this maximum efficiency is again obtained at a corresponding fluence. It has to be pointed out that the maximum value of the removal rate (4) is only obtained at this optimum point. A general expression for the removal rate of a Gaussian beam is also developed in [24,25] and reads:

$$\dot{V} = \frac{1}{4} \cdot \pi \cdot w_0^2 \cdot \delta \cdot f \cdot \ln^2\left(\frac{\phi_0}{\phi_{th}}\right) \tag{5}$$

With ϕ_0 the peak fluence in the centre of the Gaussian beam:

$$\phi(r) = \phi_0 \cdot e^{-2\cdot\frac{r^2}{w_0^2}} \quad \text{with:} \quad \phi_0 = \frac{2 \cdot E_p}{\pi \cdot w_0^2} \tag{6}$$

All these considerations clearly show that the ablation process can be optimized and that the maximum removal rate is finally given by the threshold fluence ϕ_{th} and the energy penetration depth δ. For metals and pulses longer than 10 *ps* the threshold fluence begins to increase [8-10,19]. But beside the threshold fluence also the penetration depth δ has an influence onto the maximum volume ablation rate. For pulse durations in the range from 10 *ps* to 50 *ps* the value of δ decreases with increasing pulse duration [8-10,19]. Therefore the maximum removal rate in general drops significantly down when the pulse duration is raised. The situation changes for shorter pulses. From the literature [3] one expects that the threshold fluence will rest constant when the pulse duration becomes shorter than about 10 *ps*. If these pulses would lead to higher ablation rates this can could only be caused by a higher penetration depth δ for shorter pulses.

Two remarks have to be placed here: First, Due to incubation effects the threshold fluence may strongly depend on the number of pulses applied, which is described for metals in [8,9,23,26,27]. Additionally it was found in that also the energy penetration depth shows an incubation effect of the same kind. The maximum removal rate may therefore also strongly depend on the number of pulses applied; more details are given in [8-10,23].

Second, often in the literature two different materials, pulse durations, wavelengths etc. are compared. This is normally done with identical parameters such as repetition rate, focus radius and pulse energy. But one has to have in mind that the efficiency of the ablation process is strongly influenced by the threshold fluence and the penetration depth and that these two measures depend on many parameters. Figure 1 shows the removal rate for two different sets of ϕ_{th} and δ, an average power of 1 *W* and a spot radius of 20 μm. If the ablation rates are compared at equal repetition rates the blue curve will dominate up to about 200 *kHz* and afterwards the red curve will be the more efficient one i.e. depending on the chosen repetition rate one set of parameters can be more efficient than the other and vice versa. This might be a cause that sometimes contradictory results concerning the ablation rates are reported in the literature. It becomes clear, that a fair comparison between different situations should be done by deducing the maximum ablation rate. This can be done by experimentally deducing the threshold fluence and the penetration depth.

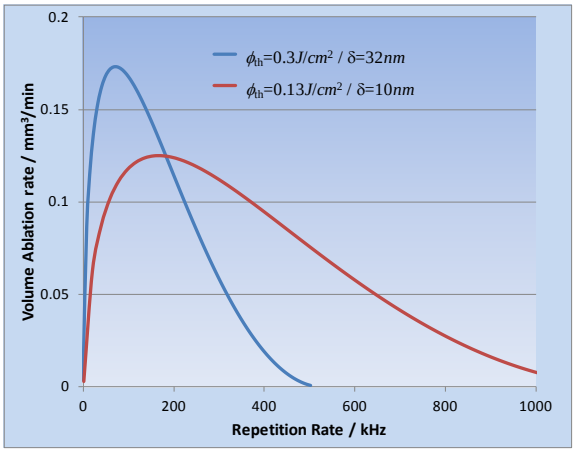

Fig 1: Removal rate for an average power of 1 *W*, a spot radius of 20 μm for two different sets of ϕ_{th} and δ.

Experimental Set-Up

The radiation of the used laser source was guided via a λ/4-plate (to generate a circular polarized beam) and folding mirrors through a beam expander into a galvo

scanning head where it was focused by an f-theta objective onto the target. For the experiments three different laser systems were used:

The experiments for 10 *ps* to 50 *ps* were performed with a DUETTO™ (Time Bandwidth Products, Switzerland) ps-laser system working at a wavelength of 1064 *nm* with a pulse duration of about 10 *ps*. By introducing corresponding etalons into the master oscillator the pulse duration was raised to 20 *ps*, 30 *ps* and 50 *ps*. The pulse duration was controlled with an autcorrelator measurement whenever the etalon was changed.

A SATSUMA (Amplitude Systemes, France) fs-laser, working at a wavelength of 1030 *nm*, was used for the experiments with pulse durations between 500 *fs* and 10 *ps* for copper, stainless steel and silicon. The pulse duration was changed from 500 *fs* to higher values by detuning the pulse compressor.

For shorter pulses and second harmonic as well, a PHAROS laser system (Light Conversion, Lithuania) was used. Here the minimum pulse duration was specified to be 223 *fs* and it could again be changed up to 10 *ps* by detuning the pulse compressor. This system was used for the experiments at 1026 *nm* and 513 *nm* for copper, silicon, germanium, ZrO_2, PCD, fused silica and soda lime glass. The frequency conversion unit was optimized for the shortest pulse durations and therefore the pulse energy in second harmonic significantly dropped down for longer pulse durations and the experiments with 513 *nm* wavelength could often only be done up to a pulse duration of 1 or 2 *ps*.

Each system included an additional picker after the last amplifier stage as a pulse on demand (POD) option to be able to reduce the repetition rate down to single pulses. Also the control of the pulse energy going with the average power was done after the last amplifier stage. It was realized with polarizer and λ/2-plates to guarantee constant beam parameters. For all different situations (laser system and wavelength) the beam quality and spot size was measured with a rotating slit beam profiler. All systems emitted a nearly Gaussian shaped beam.

In order to deduce ϕ_{th} and δ as a function of the pulse duration and the number of pulses applied, series with single ablated craters were generated for each set of these parameters, i e. 1,2,4,...,512 pulses and different pulse durations. For one series the pulse energy was raised from below up to multiples of the threshold. To avoid thermal accumulation effects the repetition rate was set to 1 *kHz* or less with the POD. The crater depths in the centre were deduced with a laser scanning microscope. These results were compared with the theoretical crater depth by introducing the peak fluence (6) into (1). The two parameters ϕ_{th} and δ were then deduced by a least square fit to the experimentally obtained data. This analysis was done for copper, steel, doped and undoped silicon and germanium. Especially at low pulse energies i.e. low fluences or low number of pulses the deduction of the crater depth became extensive and sometimes almost impossible. On the other side, too high fluences and pulse numbers lead to deep craters where it was no longer possible to measure the depth in the center.

For the semiconductors a massive crater cone formation [28] constrained the exact measurement of the crater depths. Also for the porous materials ZrO_2 and PCD as well as for the glasses the upper kind of study could not be performed with the desired accuracy. Therefore by the experiments with the PHAROS system the removal rate was additionally determined by ablating squares. The squares were built up by machining 37 hatched slices with a pulse to pulse and line distance of 8 μm for 1026 *nm* and 3 μm for 513 *nm*, respectively. The removal rate can then be deduced by measuring the depth of the square with the laser scanning microscope. Together with laser and processing parameters the removal rate can exactly be calculated. Here only the real laser on time was considered and the jump time is neglected, i.e. the calculated removal rate is a physical one and the real rate, also containing the process strategy, will be lower.

Results

Copper

For Cu-DHP (in US: C12 200) the deduced values of ϕ_{th} and δ for 128 pulses and for all pulse durations and wavelengths are summarized in Fig. 2. For the IR radiation only the second ablation regime from the two reported in [19,22] was observed. The situation changes for the green radiation where the two regimes could clearly be separated. As expected for both wavelengths ϕ_{th} do not significantly change for pulses shorter than 10 *ps*. The situation changes for δ. For IR-radiation the energy penetrations depth continuously increases with shorter pulse durations. This increase is still present for green between 10 *ps* and 1 *ps*, but it is much less pronounced and δ rests almost constant for pulses shorter than 1 *ps*.

Based on these parameters the maximum removal rate can be calculated by (4). The corresponding results are summarized in Fig. 3: For IR the removal rate continuously increases from 50 *ps* pulse duration to 500 *fs*; between 10 *ps* and 500 *fs* this increase amounts about 75% (compared to the value at 10 *ps*). For the 2nd regime in green still an increase is observed, but it only

amounts about 30%. The maximum rates for the 1st regime are much lower. Concerning the maximum removal rate the obtained values for IR and green (2nd regime) are in the same range for the pulse durations between 10 *ps* and 223 *fs* i.e. for the ablation efficiency in copper there is no advantage to go to a shorter wavelength.

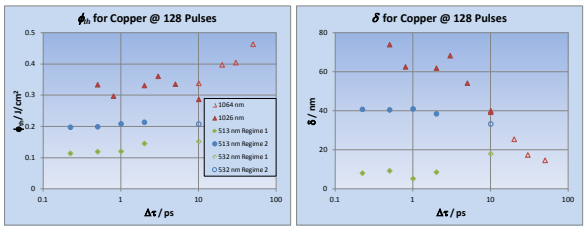

Fig. 2: Threshold fluence and penetration depth for copper as a function of the pulse duration and the wavelength.

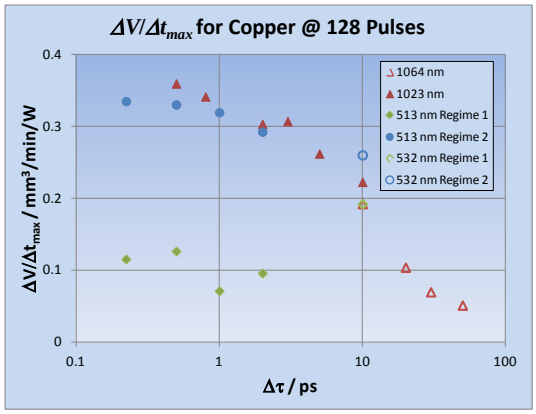

Fig. 3: Maximum removal rate for copper as a function of the pulse duration and the wavelength.

The surface quality is shown in Fig. 4; in the upper part for 1026 *nm* and in the lower part for 513 *nm*. The squares were generated with a laser repetition rate of 200 *kHz* and a peak fluence (6) of about 0.85 J/cm^2 for 1026 *nm* and 513 *nm* as well. The spot radius amounted 19.5 μm for 1026 *nm* and 7.5 μm for 513 *nm*. Due to the decreasing conversion efficiency the pulse duration was limited to 2 *ps* for 513 *nm*. As it can be seen from the SEM-pictures the surface quality is not affected by the pulse duration, neither for 1026 *nm* nor for 513 *nm*. For the green wavelength the surface roughness seem to be better compared to IR but this is mainly explained by the smaller focus radius and hatch distance.

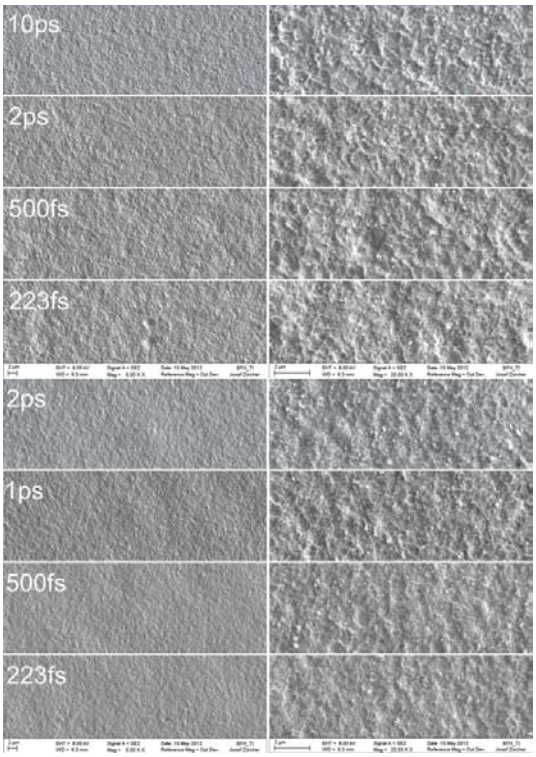

Fig. 4: Surface of ablated squares in copper for 1026 *nm* (up) and 513 *nm* (below).

Stainless Steel

Stainless steel 1.4301 (in US: AISI 304) was only investigated for a wavelength of 1064 *nm* between 10 *ps* and 50 *ps* and for 1030 *nm* between 10 *ps* and 500 *fs*. Fig. 5 shows the results of the study for 256 pulses. For long ps-pulses ϕ_{th} strongly depends on the pulse duration. For pulse durations equal or shorter than 10 *ps* ϕ_{th} rests again constant. In contrast δ significantly drops when the pulse duration is raised from 500 *fs* to 10 and 20 *ps*. For longer pulses this drop is stopped and δ even slightly raises for a pulse duration of 50 *ps*. This small increase could be an indication that for this pulse duration the conventional heat conduction begins to dominate the energy transport in the material. In this regime ϕ_{th} and δ are expected to depend on the square root of the pulse duration.

From these values again the maximum removal rate (4) is calculated and shown in Fig. 6. As for copper the removal rate increases with decreasing pulse duration. Compared to the value at 10 ps it amounts only about 20% at 50 *ps*, a strong drop. In contrast for the pulse duration of 500 *fs* an increase of about 65% is obtained.

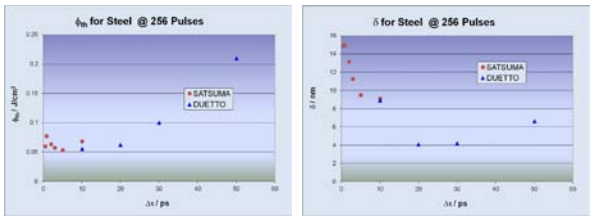

Fig. 5: Threshold fluence and energy penetration depth for stainless steel as a function of the pulse duration.

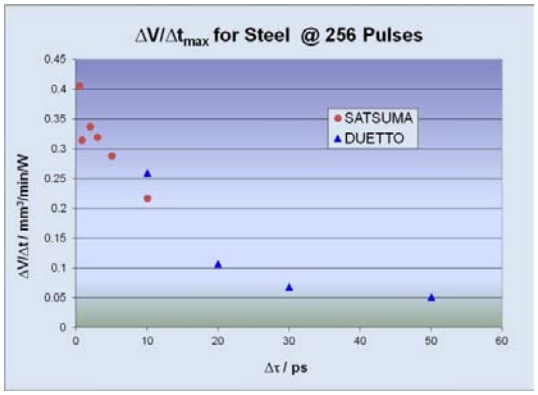

Fig. 6: Maximum removal rate for stainless steel as a function of the pulse duration.

Fig. 7 shows the SEM image with detail view of marked lines machined with an average power of 170 *mW*, a spot radius of 13.5 *µm*, a repetition rate of 100 *kHz*, a marking speed of 160 *mm/s* and 15 repeats. Please note that the scale for the upper images differs for 10 *ps* and 500 *fs* and the apparent smaller line width for 500 *fs* is due to this different scale. In the lower detail view small "worms of melted material" are observed between the ripples. These "worms" are much less pronounced for the pulse duration of 500 *fs*.

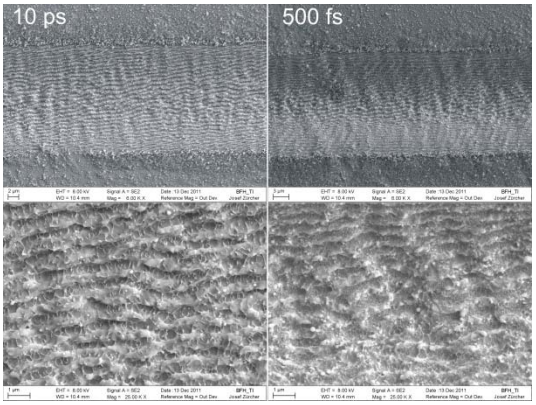

Fig. 7: SEM images with detail view of marked lines in steel.

Undoped Silicon

For undoped silicon again an almost constant ϕ_{th} is observed for 1030 *nm*. For 513 *nm* the threshold seems to have a tendency to lower values at shorter pulse durations but this is not confirmed by the other numbers of applied pulses. For both wavelengths the penetration depth δ increases with decreasing pulse duration. This behaviour will again lead to an increased removal rate for shorter pulse durations which is confirmed, see Fig. 9, by the obtained removal rates from the ablated squares. Here the wavelength of 513 *nm* is more efficient. Introducing the values of the threshold and the penetration depth into (4) will lead to a contrary result were the IR radiation should show higher removal rates. The reason for this difference is not clear yet and further investigations have to be done.

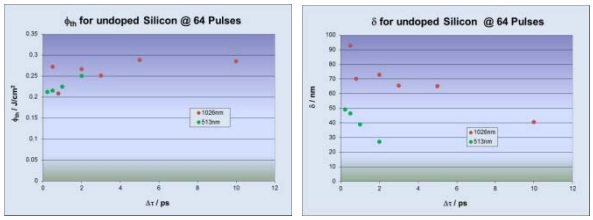

Fig. 8: Threshold fluence and energy penetration depth for undoped silicon.

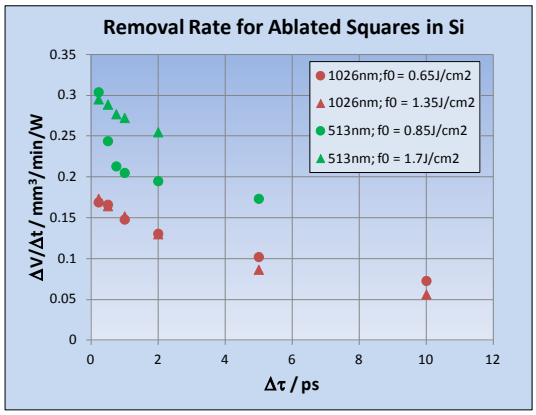

Fig. 9: Removal rate obtained from the ablated squares for the different wavelengths and two different fluences.

The pulse durations has also an influence onto the crater and cone formation at the bottom of the ablated squares, as shown in Fig.10. Theses squares were generated with a repetition rate of 100 *kHz* and a peak fluence of about 2.7 J/cm^2 (left) and 5.3 J/cm^2 (right). For a pulse duration of 10 *ps* the surface is flat for both fluences. For the higher fluence the crater and cone formations starts at a pulse duration of about 5 *ps*

whereas it is already present for the lower fuence. For lower pulse durations the crater and cone formation seems to be unaffected. The fluence has an influence onto the dimensions of the crater and cones in the way that higher fluences lead do bigger cones.

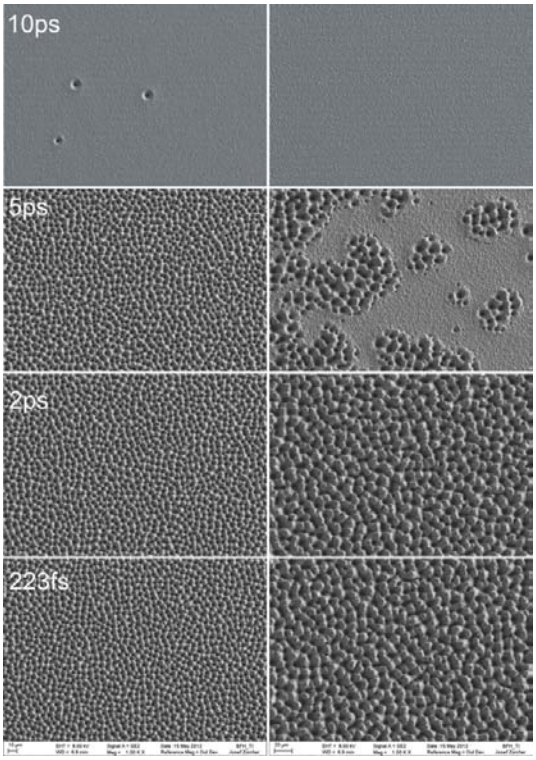

Fig. 10: Surface of the ablated squares in undoped silicon for different pulse durations and peak fluencies; left: 2.7 J/cm^2 right: 5.3 J/cm^2

Germanium

The threshold fluence ϕ_{th} and the penetration depth δ were only investigated for 513 *nm* and pulse durations between 223 *fs* and 2 *ps*. The results show the same tendency as already obtained for silicon e.g. for 64 pulses the threshold fluence is in the range of 0.2 J/cm^2 and the penetration depth changes from 80 *nm* to 120 *nm* when the pulse duration is reduced from 2 *ps* to 223 *fs*. The corresponding maximum removal rates are between 0.75 and 0.9 $mm^3/min/W$ which is about twice the value from silicon. This higher value is also confirmed by the removal rate measured from the ablated squares shown in Fig. 11. The increase in the ablation rate for shorter pulse durations is still present but is much less pronounced than for silicon and again for 513 *nm* the removal rate is up to 2 times higher than for 1026 *nm*.

In contrast to silicon, crater and cone formation is also observed for the pulse duration of 10 *ps*. This is illustrated in Fig.12 for the peak fluences of 4 J/cm^2, 2.7 J/cm^2, 1.35 J/cm^2 and 0.67 J/cm^2 and the pulse durations of 223 *fs* (left) and 10 *ps* (right). The same dependence of the cone dimension on the fluence as for silicon is observed. For the two high fluences some kind of small deep holes in the cones are observed for 223 *fs* pulse duration.

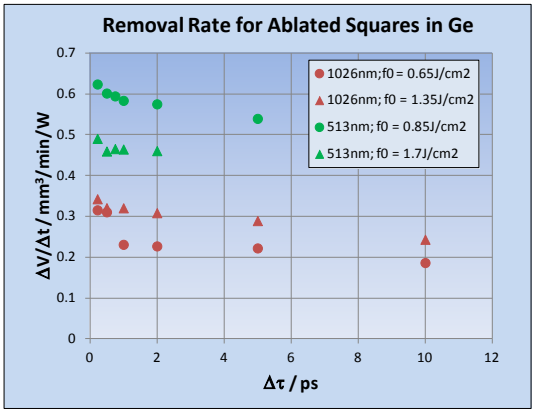

Fig. 11: Removal rate obtained from the ablated squares for the different wavelengths and two different fluences.

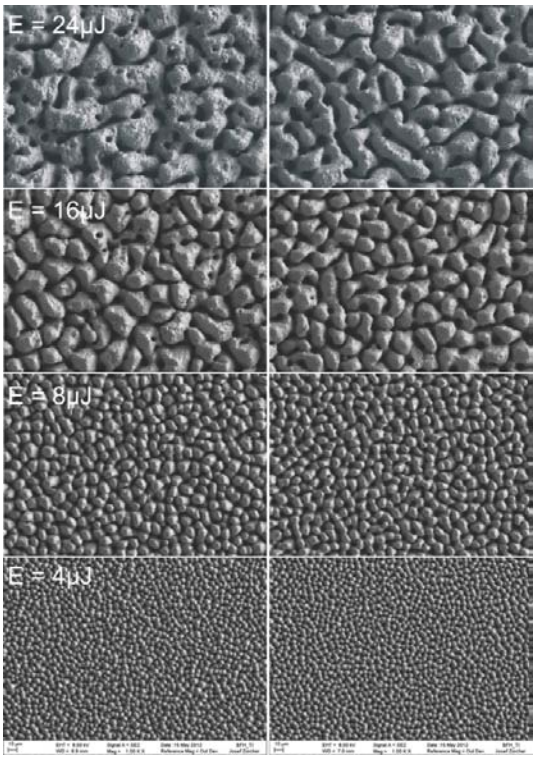

Fig. 12: Surface of the ablated squares in germanium for 223 fs (left) and 10 ps (right) pulses and the four peak fluencies (top down) 4 J/cm^2, 2.7 J/cm^2, 1.35 J/cm^2 and 0.67 J/cm^2.

PCD

For pulse durations shorter than 10 *ps* the removal rate was only deduced via the ablated squares and the values are compared with the ones obtained from earlier work [10] (see Fig. 13). For IR radiation a continuous increase is observed when the pulse duration is reduced from 50 *ps* to 223 *fs*. This increase is higher for ps pulses and becomes low in fs regime. For 513 *nm* the removal rate rests almost constant and equals the one obtained for 1023 *nm*. In general the obtained removal rate is very low compared to other materials. Almost no difference in the surface quality was observed in the full range of the investigated pulse durations.

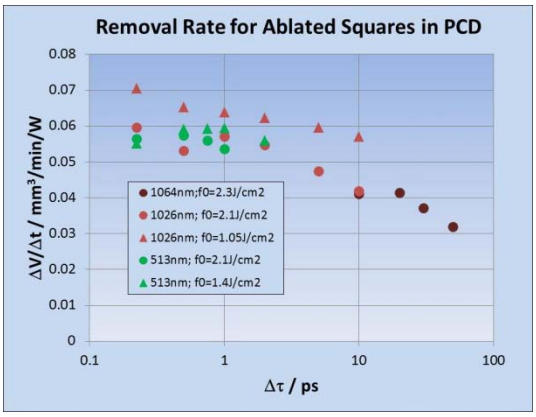

Fig. 13: Removal rates from ablated squares for PCD.

ZrO_2

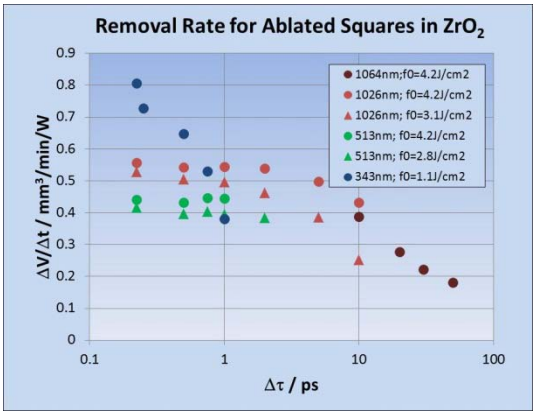

Fig. 14: Removal rates from ablated squares for ZrO_2

Also for ZrO_2 the removal rates were deduced via the ablated squares and compared with former results (see Fig.14). For IR radiation a strong increase of the removal rate between 10 *ps* and 50 *ps* was observed, followed from the region between 10 *ps* and 1 *ps* with a moderate increase. For shorter pulses no increase is observed any more. For 513 nm almost no change of the removal rate can be seen between 2 *ps* and 223 *fs*. In contrast for UV radiation an about two times higher value of the removal rate at 223 *fs* compared to 1 *ps* is obtained, but at a fluence value which is low compared to the other wavelengths.

Glasses

Soda lime glass

Soda lime glass shows a completely different behaviour as illustrated in Fig. 15. Here the removal rate was deduced from the ablated squares. For short pulses the removal rate is small, in the range of 0.1-0.2 $mm^3/min/W$. When the pulse duration is raised, a rapid changeover into a second regime with a much higher removal rate is observed. The pulse duration when this changeover happens depends on the wavelength and the peak fluence. For 513 *nm* it amounts about 310 *fs* for $\phi_0 = 4.2\ J/cm^2$ and 400 *fs* for $\phi_0 = 5.7\ J/cm^2$. For 1026 *nm* the corresponding values are 660 *fs* for $\phi_0 = 3.1\ J/cm^2$ and 940 *fs* for $\phi_0 = 4.2\ J/cm^2$. After reaching the maximum value the removal rate is continuously dropping down to zero when the pulse duration is further raised. For 1026 *nm* no ablation was observed for 10 *ps* and $\phi_0 = 4.2\ J/cm^2$ or for 5 *ps* and $\phi_0 = 3.1\ J/cm^2$. For 513 *nm* the pulse duration was limited to values equal or lower than 1 *ps* because the desired pulse energy could not be reached for higher pulse durations. Therefore it was not possible to deduce how the rate drops after reaching its maximum value.

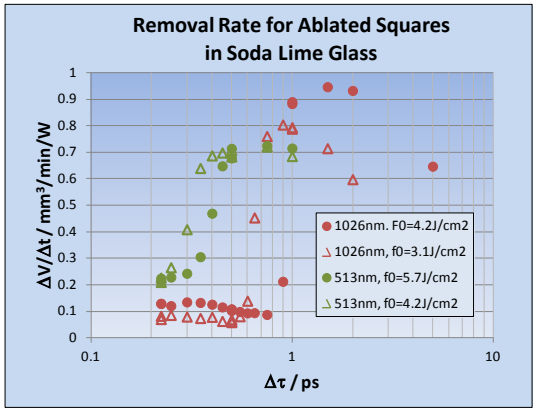

Fig. 15: Removal rates for 1026 *nm* and 513 *nm* from ablated squares for soda lime glass.

Fig. 16 shows SEM images for 1026 *nm* and $\phi_0 = 4.2\ J/cm^2$ for the shortest pulse durations of 223 *fs*, at 750 *fs* where the removal rate begins to increase, at the edge of the increase (900 *fs*) and at 1 *ps* shortly before the removal rate reaches its maximum

value. Huge differences of the surface are observed. For 223 *fs* and 750 *fs* the bottom surface of the ablated squares is flat with a low roughness, shown on the right side of Fig. 16. For 223 *fs* the bottom is covered by melted particles with sizes of less than *500 nm* and by melting splashes. For 750 *fs* the number of particles and splashes is much reduced. The overview on the left side shows small cracks in the surface. For 900 *fs* two different ablation regimes are observed at the same time. In the first one the surface equals the ones from 223 and 750 *fs* whereas in the second one the surface becomes significantly rougher and also porous. It looks like particles with dimensions higher than 1 μm were somehow "sintered". This type of surface equals the ones obtained for pulse durations of 1 *ps* and more where the removal rate is now enlarged by about a factor of 7 compared to the short pulse durations. The cracks in the surface observed for 750 *fs* and 223 *fs* may still be present but can't be detected as easy as before. Similar results have been obtained for the wavelength of 513 *nm*. Further investigations have o be done to clarify the corresponding ablation processes.

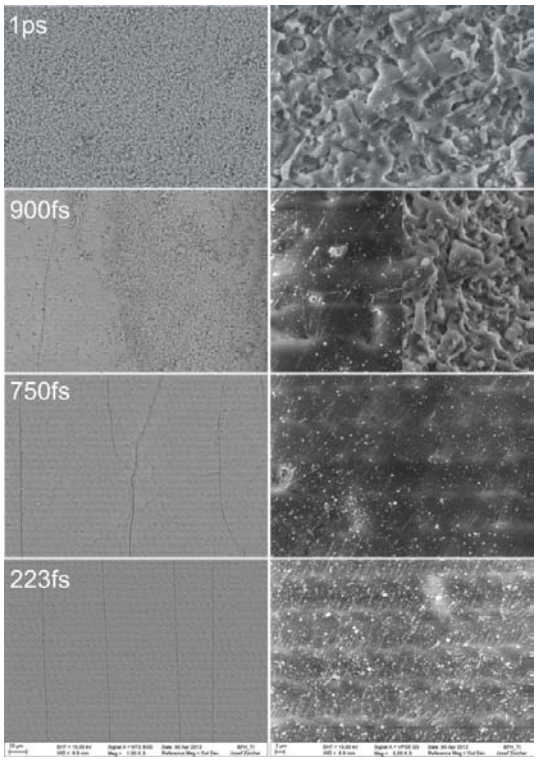

Fig. 16: SEM images of surfaces obtained at the wavelength 1026 *nm* for soda lime glass with a peak fluence of 4.2 J/cm^2. Left: overview; Right: Detail

Fused Silica

Squares were machined into 1 *mm* thick fused silica for different pulse durations and wavelengths. The removal rates were in the range between 0.25 and 0.45 $mm^3/min/W$ and did not show such a high dependence on the pulse duration compared to soda lime glass as shown in Fig. 17. Again it was not possible to get pulses longer than 1 *ps* with the desired fluence for 513 *nm*. At the wavelength of 1026 *nm* and for 2 *ps* and $\phi_0 = 3.1\ J/cm^2$ or 5 *ps* and $\phi_0 = 4.2\ J/cm^2$ the location of the ablation process moved from the front side to the back side due to self-focusing.

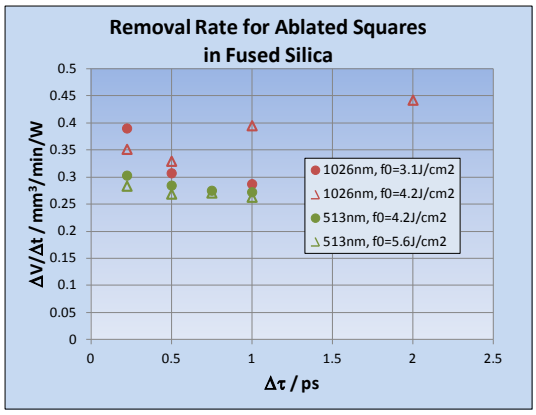

Fig. 17: Removal rates for 1026 *nm* and 513 *nm* from ablated squares for fused silica.

The surface of the ablated squares for 513 *nm* and $\phi_0 = 4.2\ J/cm^2$ are shown in Fig. 18. For all pulse durations the surface looks porous and again like particles were sintered. In contrast to soda lime glass the particle dimension here is only a few 100 *nm*. Similar surfaces were also observed for 1026 *nm*.

Conclusion

For several materials the influence of the pulse duration onto the removal rate was investigated. All materials, except the glasses, show a tendency to higher removal rates when the pulse duration is decreased from 10 *ps* to 500 *fs* or 223 *fs*. For the investigated metals copper and steel as well as for silicon and germanium, this growth can be explained by an increased energy penetration depth for shorter pulses. Compared to 1 μm radiation the increase of the removal rate may be less pronounced as observed for copper, ZrO_2 and PCD. For copper the surface quality is almost independent from the pulse duration whereas for steel better surface qualities are observed for fs pulses. For semiconductors a strong crater and cone formation was observed. For silicon the appearance of the cones can be influenced by the pulse duration, but its dimensions are affected form the applied fluence

and not from the pulse duration. For ZrO_2 and PCD no dependence of the surface quality on the pulse duration was observed, also for pulse durations from 10 *ps* to 50 *ps*.

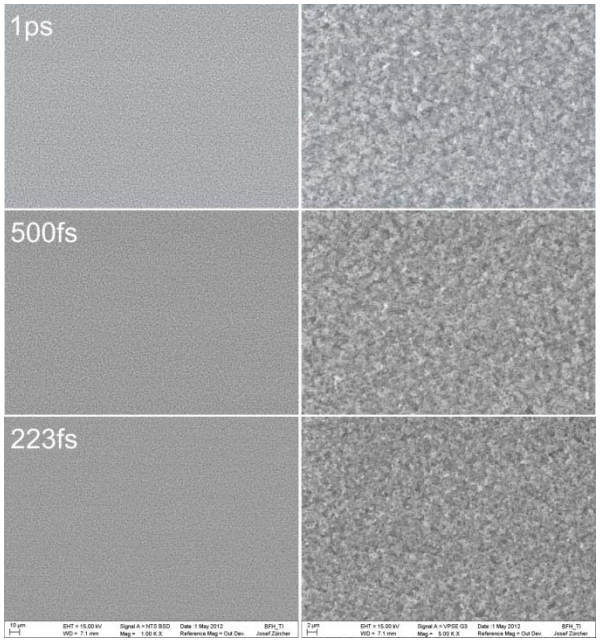

Fig. 18: SEM images of surfaces obtained at the wavelength 513 nm for fused silica with a peak fluence of 4.2 J/cm^2. Left: overview; Right: Detail

A very interesting dependence on the pulse duration was observed for soda lime glass. Here the removal rate shows a sharp edge to significantly higher values when the pulse duration is raised from fs towards ps. The two regimes separated by this sharp edge shows completely different surface qualities. For short pulses going with low removal rates the surface is flat and covered by malted particles and splashes. For higher pulse durations, going high removal rates, the surface looks like to be covered by sintered particles. This is also the type of surface quality which was observed for fused silica and all investigated pulse durations.

For all materials a pulse duration around 1 *ps* seems to be a good choice concerning the removal rate and the surface quality.

Acknowledgements

The authors wish to thank Josef Zuercher for his help with the SEM images. This work was supported by the Swiss Commission for Technology and Innovation CTI.

References

[1] B. N. Chichkov, C. Momma, S. Nolte, F. von Alvensleben and A. Tünnermann, „Femtosecond, picosecond and nanosecond laser ablation of solids“, Appl. Phys. A 63, 109 (1996).

[2] Detlef Breitling, Andreas Ruf and Friedrich Dausinger, “Fundamental aspects in machining of metals with short and ulrashort laser pulses”, Proc. SPIE 5339, 49-63 (2004)

[3] Friedrich Dausinger, Helmut Hügel and Vitali Konov, “Micro-machining with ultrashort laser pulses: From basic understanding to technical applications”, Proc. SPIE Vol. 5147, 106-115 (2003)

[4] J. Meijer, K. Du, A. Gillner, D. Hoffmann, V. S. Kovalenko, T. Masuzawa, A. Ostendorf, R. Poprawe, W. Schulz, “Laser Machining by Short and Ultrashort Pulses – State of the Art”, Annals of the CIRP, 51/2 (2002)

[5] S. Pierrot, J. Saby, B. Cocquelin and F. Salin, “High-Power all Fiber Picosecond Sources from IR to UV”, Proc. of SPIE Vol. 7914, paper 79140Q (2011)

[6] S. Kanzelmeyer, H. Sayinc, T. Theeg, M. Frede, J. Neumann and D. Kracht, “All-fiber based amplification of 40 ps pulses from a gain-switched laser diode”, Proc. of SPIE Vol. 7914, paper 191411 (2011)

[7] P Deladurantaye, A. Cournoyer, M. Drolet, L. Desbiens, D. Lemieux, M. Briand and Y. Taillon, “Material micomachining using bursts of high repetition rate picoseconds pulses from a fiber laser source”, Proc. of SPIE Vol. 7914, paper 791404 (2011)

[8] M. Schmid, B. Neuenschwander, V. Romano, B. Jaeggi and U. Hunziker, "Processing of metals with ps-laser pulses in the range between 10ps and 100ps", Proc. of SPIE Vol. 7920, paper 792009 (2011)

[9] B. Jaeggi, B. Neuenschwander, M. Schmid, M. Muralt, J. Zuercher and U. Hunziker, "Influence of the Pulse Duration in the ps-Regime on the Ablation Efficiency of Metals", Physics Procedia 12, 164-171 (2011)

[10] B. Neuenschwander, B. Jaeggi, M. Schmid, U. Hunziker, B. Luescher, C. Nocera, "Processing of industrially relevant non metals with laser pulses in the range between 10 ps and 50 ps", ICALEO 2011, Paper M103 (2011)

[11] B. Sallé, O. Gobert, P. Meynadier, G. Petite and A. Semerok, "Femtosecond and picosecond laser microablation: ablation efficiency and laser microplasma expansion", Appl. Phys. A 69[Suppl.], 382 – 383 (1999)

[12] R. Le Harzig, D. Breitling, M. Weikert, S. Sommer, C. Föhl, S. Valette, C. Donnet, E. AUdouard and F. Dausinger, "Pulse width and energy influence on laser micromachining of metals in a range of 100 fs to 5 ps", Appl. Surf. Science 249, 322-331 (2005)

[13] J. Lopez, A. Lidolff, M. Delaigue, C. Hönninger, S. Ricaud and E. Mottay, "Ultrafast Laser with highEnergy and high average power for Industrial Micromachining: Comparision ps-fs", ICALEO 2011, Paper 401 (2011)

[14] O. Utéza, N. Scanner, B. CVhimier, M. Sentis, P. Lassonde, F. Légardé and J.C. Kieffer, "Surface Ablation od Dielectrics with sub-10 fs to 300 fs Laser Pulses : Crater Depth and Diameter, and Efficiency as a Function of Laser Intensity", JLMN-J. of Laser Micro/Nanoengineering, Vol. 5, No. 3, 238-241 (2010)

[15] P. Russbueldt, T. Mans, J. Weitenberg, H.-D. Hoffmann, R. Poprawe, "Compact diode-pumped 1.1 kW Yb:YAG Innoslab femtosecond amplifier," Opt. Lett. 35, 4169-4171 (2010)

[16] P. Russbueldt, T. Mans, H-D. Hoffmann, R. Poprawe, "1100 W Yb:YAG femtosecond Innoslab amplifier", Proc. of SPIE, 7912 (2011)

[17] C. Momma, B.N. Chichkov, S. Nolte, F. van Alvensleben, A. Tünnermann, H. Welling and B. Wellegehausen, "Short-pulse laser ablation of solid targets", Opt. Comm. 129, 134-142 (1996)

[18] C. Momma, S. Nolte, B.N. Chichkov, F. van Alvensleben and A. Tünnermann, "Precise laser ablation with ultrashort pulses", Appl. Surf. Science 109/110, 15-19 (1997)

[19] S. Nolte, C. Momma, H. Jacobs, A. Tünnermann, B.N. Chichkov, B. Wellegehausen and H. Welling, "Ablation of metals by ultrashort laser pulses", J. Opt. Soc. Am. B, Vol. 14, No. 10 (1997)

[20] S.I. Anisimov and B. Rethfeld, "On the theory of ultrashort laser pulse interaction with a metal", Proc. SPIE 3093, 192-203 (1997)

[21] B.H. Christensen, K. Vestentofrt and P. Balling, "Short-pulse ablation rates and the two-temperature model", Appl. Surf. Science 253, 6347-6352 (2007)

[22] P. Mannion, J. Magee. E. Coyne and G.M. O'Conner, "Ablation Thresholds in ultrafast laser micro-machining of common metals in air", Proc. of SPIE vol. 4876, 470-478 (2002)

[23] B. Neuenschwander et al., "Optimization of the volume ablation rate for metals at different laser pulse-durations from ps to fs", Proc. of SPIE vol. 8243, 824307-1 (2012)

[24] B. Neuenschwander, G. Bucher, C. Nussbaum, B. Joss, M. Muralt, U. Hunziker et al., "Processing of dielectric materials and metals with ps-laserpulses: results, strategies limitations and needs", Proceedings of SPIE vol. 7584, (2010)

[25] G. Raciukaitis, M. Brikas, P. Gecys, B. Voisiat, M. Gedvilas, "Use of High Repetition Rate and High Power Lasers in Microfabrication: How to keep Efficiency High?", JLMN Journal of Laser Micro/Nanoengineering, Vol. 4 (3), 186-191 (2009)

[26] Y. Jee, M.F. Becker and R.M. Walser, "Laser-induced damage on single-crystal metal surfaces", J. Opt. Soc. Am. B5, (1988)

[27] P.T. Mannion, J. Magee, E. Coyne, G.M. O'Connor and T.J. Glynn, "The effect of damage accumulation behavior on ablation thresholds and damage morphology in ultrafast laser micro-machining of common metals in air", Appl. Surface Science 233, 275 – 287 (2004)

[28] D. H. Lowndes, J. D. Fowlkes and A. J. Pedraza, "Early stages of pulsed-laser growth of silicon microcolumns and microcones in air and SF_6", Appl. Surface Science 154-155, pp 647 – 658 (2000)